Annu. Rev. Phys. Chem. 2004. 55:197–229
doi: 10.1146/annurev.physchem.54.011002.103833

First published online as a Review in Advance on February 3, 2004

ADSORPTION AND REACTION AT ELECTROCHEMICAL INTERFACES AS PROBED BY SURFACE-ENHANCED RAMAN SPECTROSCOPY

Zhong-Qun Tian[1] and Bin Ren[2]
[1]*State Key Laboratory for Physical Chemistry of Solid Surfaces, Xiamen University, Xiamen, 361005, China; email: zqtian@xmu.edu.cn*
[2]*Department of Chemistry, Xiamen University, Xiamen, 361005, China; email: bren@jingxian.xmu.edu.cn*

Key Words confocal Raman microscopy, time-resolved measurement, hydrogen adsorption, methanol oxidation, interfacial water

■ **Abstract** Over the past three decades, surface-enhanced Raman spectroscopy (SERS) has gone through a tortuous pathway to develop into a powerful surface diagnostic technique for in situ investigation of surface adsorption and reactions on electrodes. This review presents the recent progress achieved mainly in our laboratory on the improvement of detection sensitivities as well as spectral, temporal, and spatial resolutions. Various surface roughening procedures for electrodes of different metals coupled with maximum use of a high-sensitivity confocal Raman microscope enable us to obtain good-quality SER spectra on the electrode surfaces made from net Pt, Ni, Co, Fe, Pd, Rh, Ru, and their alloys that were traditionally considered to be non-SERS active. A novel technique called potential-averaged SERS (PASERS) has been developed for the quantitative study of electrochemical sorption. Applications are exemplified on extensively studied areas such as coadsorption, electrocatalysis, corrosion, and fuel cells, and several advantages of in situ electrochemical SERS are demonstrated. Finally, further developments in this field are briefly discussed with emphasis on the emerging methodology.

INTRODUCTION

The structure and dynamics of electrode/liquid interfaces play an increasingly important role in electrochemistry. Ramifications of the subject matter extend into areas as diverse as batteries, fuel cells, material corrosion, clean technology, semiconductor processing, electric synthesis, conversion and storage of solar energy, and biological electron transfer processes (1–3). Conventional electrochemical methods have reached their limit in meeting the growing requirements of characterizing complex and sophisticated systems, for example, those related to advanced materials and life sciences. Since the 1980s there have been remarkable developments

of nonelectrochemical techniques to gain more mechanistic and dynamic information on electrochemical interfaces at the molecular (and/or atomic) level by the in situ mode (1, 4–6). Vibrational spectroscopic methods such as infrared (IR) (7, 8), Raman (9–11), and sum frequency generation (SFG) have been widely employed to identify the molecules and the nature of the chemisorption bond (12, 13). Second harmonic generation (SHG) (13, 14) and electroreflectance spectroscopy (15) in the visible and UV ranges have provided information about the orientation of adsorbed molecular overlayers, as well as on states, composition, and structure of electrode surfaces. X-ray absorption spectroscopy, particularly that coupled with a synchrotron source, has been employed to determine the coordination numbers of adsorbed species, the substrate-adsorbate bond lengths, and surface structures (16). Scanning probe microscopy (SPM) has provided much information concerning the microstructure and surface dynamics of both electrode and surface species (17, 18). Neutron reflectometry (NR) as a relatively new technique has been applied successfully in determining the detailed structure of monolayers and bilayers of surfactants as well as thin organic films deposited at the electrode/solution interface (19, 20). These impressive advances have been accompanied by parallel progress in quantitative electrochemical investigations based on thermodynamic measurements of capacitance, charges, and surface stresses (21, 22). Thus, the basic data such as adsorption isotherms and free energies of adsorption for adsorbates can be correlated with the spectroscopic results (3, 23). As a result, combined developments, especially in the past decade, culminate in producing a wealth of excellent information leading to a better understanding of the complexity of interfacial electrochemistry.

It should be pointed out that each technique alone has its strengths and limitations in the study of a certain electrochemical system. The detection sensitivity and resolution are two very important criteria for comparing these techniques in terms of their capability in providing high quality information from interfaces. The resolution can be further classified into energy-resolution, spatial-resolution, and time-resolution. For this purpose, a brief comparison of several widely used techniques in electrochemistry is listed in Table 1. As shown in the Table, the detection sensitivity is the most important issue because only an extremely small quantity of species providing meaningful information is present at the surface in comparison to an overwhelmingly large amount of the same species existing in the bulk solution. Existing electrochemical techniques generally have a very high sensitivity capable of detecting a molecular or atomic change in the interface at the submonolayer quantity. However, they have a poor time resolution at milliseconds unless microelectrodes or ultra-microelectrodes are used. The latter may be capable of reaching a resolution up to microseconds or even nanoseconds. Moreover, their energy-resolution is even poorer at around 10^{-2} V. In contrast, in situ vibrational spectroscopy has a much higher energy-resolution, the spectral resolution of which can easily achieve $\sim$1 cm^{-1}, which is equal to about 10^{-4} eV with excitation in the visible light region. Such a powerful technique is capable of providing much more detailed structural information, for example, to qualitatively

TABLE 1 A comparison of the sensitivity, and energetic, time and spatial resolution of electrochemical methods, Raman spectroscopy and scanning tunneling microscopy (STM) in practical electrochemistry study

	Electrochemistry	**EC-Raman spectroscopy**	**EC-STM**
Sensitivity	Submonolayer	Submonolayer[a]	Submonolayer
Energetic resolution	10^{-2} V	10^{-4} eV($\sim$1 cm^{-1})[b]	STS is not available[c]
Spatial resolution	1μm[d]	1 μm	1 Å
Time resolution	10^{-6} s	10^{-8} s[e], 10^{-3} s[f]	0.04 s[g]

[a]With the surface-enhanced Raman spectroscopy; [b]with excitation in the visible light; [c]scanning tunneling spectroscopy; although inelastic electron tunneling spectroscopy provides higher resolution at about 0.05 eV at very low temperatures (several Kelvin), it is not practical for electrochemistry; [d]with the use of scanning electrochemical microscopy; [e]with the use of pulsed laser; [g]0.04 s per STM image.

determine surface bonding, conformation, and orientation; these in turn, provide new and powerful insights into various electrochemical interfaces.

Raman spectra can be obtained by using excitation ranging from ultraviolet (UV) to near-IR energies. Water, the most important solvent in electrochemistry, is a very weak Raman scatterer and has almost no absorption in the visible light region. More importantly, Raman spectroscopy can be conveniently applied not only to in situ measurements of solid-liquid interfaces in fundamental as well as practical studies (9–11), but also to the porous and rough surfaces with high surface areas that are very difficult to study using many other surface techniques. Furthermore, Raman spectroscopy has a wide spectral window (5 cm^{-1} $\sim$ 4000 cm^{-1}), and requires neither complicated sample preparations nor special cell materials. All these advantages make Raman spectroscopy a more convenient and powerful tool for analysis of an electrode/aqueous solution interface. However, this promising technique for interfacial electrochemistry has encountered difficulties due to its intrinsically low-detection sensitivity. Since the cross section of a molecule for the Raman process is about 10^6 and 10^{14} times smaller than those of infrared and fluorescence processes, respectively (11), the intensity of typically 10^{-8} to 10^{-10} of the incident photon flux is not sufficient to detect surface adsorbate with (sub)monolayer coverage.

The first in situ Raman spectroscopic study on an electrochemical system was reported by Fleischmann et al. (24) in 1973 on thin Hg_2Cl_2, Hg_2Br_2, and HgO films formed on mercury droplets electrodeposited on platinum electrodes. These compounds have exceptionally large Raman scattering cross sections (i.e., very good Raman scatters) so that a signal from a species as little as a few monolayers could be detected on a high-surface-area electrode. The experiment proved the viability of in situ Raman spectroscopic measurements under electrochemical environments. Soon after, Van Duyne and coworkers (25) obtained Raman signals of electrochemically generated radical ions both in the bulk electrolyte and the diffusion layer. As the normal Raman scattering was too weak to be measured for

those species in the thin diffusion layer, they used resonance Raman spectroscopy to enormously boost the detection sensitivity.

The landmark breakthrough in the development of electrochemical Raman spectroscopy was the realization of studies of adsorbed and reaction species at electrode surfaces. In the mid-1970s, largely through the contribution of the groups of Fleischmann and Van Duyne (26, 27), it was discovered that molecules adsorbed on a specially prepared silver surface produce a Raman spectrum that is at times a millionfold more intense than expected. This effect was dubbed as surface-enhanced Raman scattering (SERS) (28). This observation opened up a great opportunity to design highly sensitive surface diagnostic techniques applicable to electrochemical, biological, and other ambient interfaces.

In spite of the fact that thousands of papers on SERS have been published, the development of SERS into a widely used tool has been slow. For two decades there had been two major obstacles hampering the development of electrochemical SERS (EC-SERS)**.** First, only three noble metals (Au, Ag, and Cu) provide the large enhancement needed, which severely limited the range of SERS's practical applications. Whereas transition metals have much wider application in electrochemistry, they have been commonly considered as non-SERS-active substrates. Second, the high SERS-active substrates normally suffer from instability, which leads to poor reversibility during EC-SERS measurements. As a consequence, it is difficult to quantitatively correlate the electrochemical data with SERS intensity. Overall, SERS has not gained as wide usage as IR spectroscopy has in surface science and electrochemistry.

This review aims to present our contributions in recent years: First, how to extend SERS into a widely applicable and powerful technique, and second, to discuss broad applications of SERS to the study of electrode adsorption and reactions. The review is organized in three sections as follows: In the first section, three approaches are described with emphasis on experimental methodology, such as how to fully exploit the strengths and offset shortcomings of SERS as applied in surface electrochemistry. In the second section, the SERS investigations on electrochemical adsorption and reaction are presented with emphasis on spectral resolution, temporal resolution, and/or spatial resolution. In the final section, prospects and further developments in electrochemical SERS techniques are briefly discussed. For readers interested in comprehensive aspects of SERS, excellent review articles and special issues describing details of various aspects of the subject, including single-molecule SERS, are recommended (28–32). There are also some excellent reviews focused on the electrochemical applications of SERS prior to the mid-1990s (9–11).

DEVELOPMENT OF ELECTROCHEMICAL SERS

Generating SERS Directly on Transition Metal Electrodes

Up until the mid-1970s, the biggest challenge to the development of EC-SERS techniques was to generate SERS directly on transition metals because it was

commonly accepted that transition metals were not SERS active. During the next two decades, scientists devised various strategies to meet that challenge (33–36) with limited success. The reported surface spectra were obtained either only under optimal conditions or by data manipulation using a spectral subtraction method even though these surface Raman signals were too weak to be investigated in detail. Worse still, some results could not be repeated by other groups.

To bypass the aforementioned obstacle, Weaver et al. and Fleischmann et al. independently developed a "borrowing SERS" strategy (37–40) by depositing an ultrathin transition-metal layer over a SERS-active surface. With the aid of the long-range effect of the electromagnetic enhancement (28–31) created by the high SERS-active substrate underneath, good-quality SERS spectra of adsorbates on several transition metal films have been obtained. Recently, the pinhole problem of the ultrathin film has been overcome by Weaver and his coworkers using the "pinhole-free" tactic (41–48). However, this method still has the other two problems: the stability of the film under vigorous electrochemical conditions and the difference between the crystalline structure of the films and the massive metals. Furthermore, the "borrowing SERS" strategy is based on the notion that transition metals do not exhibit SERS. Apparently, these results did not strongly support SERS viability and feasibility on pure massive transition metal surfaces.

This notion has been turned around since the late 1990s. It was demonstrated convincingly that SERS could be generated directly on the electrode surfaces made from massive transition metals and their alloys (49–53). This advance was made possible primarily owing to the development of various methods for fabricating nanostructured surfaces and the optimization of confocal Raman microscope performance (54–56).

From the SERS studies on Au, Ag, and Cu, it has been well known that a necessary requirement for the presence of great surface enhancement is proper surface roughness, or more exactly, nanostructured surfaces. Five SERS activation procedures have been developed for different transition metals, i.e., potential-controlled ORC (49), current-controlled ORC (57), chemical etching (50, 51), electrodeposition (52), and template synthesis (58, 59). Figure 1 demonstrates the distinct effect on the Raman intensity of pyridine adsorbed on Fe electrode surfaces produced by surface roughening procedures. When the surface was mechanically polished with fine-grade alumina powders of 0.3 μm, the only Raman signal registered was solely from both pyridine and water in the bulk solution as shown in Figure 1*a*. This spectrum serves as the reference. The signal of pyridine adsorbed on surfaces could be detected after the electrode was chemically etched in 2.0 M H_2SO_4 (Figure 1*b*). The signal intensity increased if the electrode was further treated in a 0.5 M solution of H_2SO_4 by a double-step ORC (Figure 1*c*). An even more intense signal was obtained when an additional ORC was performed in situ in a spectroelectrochemical cell prior to measurement. A broad band at around 240 cm^{-1} assigned to the Fe-N vibration can be clearly observed, as shown in Figure 1*d*. This example reveals the importance of preparing appropriate surface morphology for generating optimum surface enhancement. Using the template

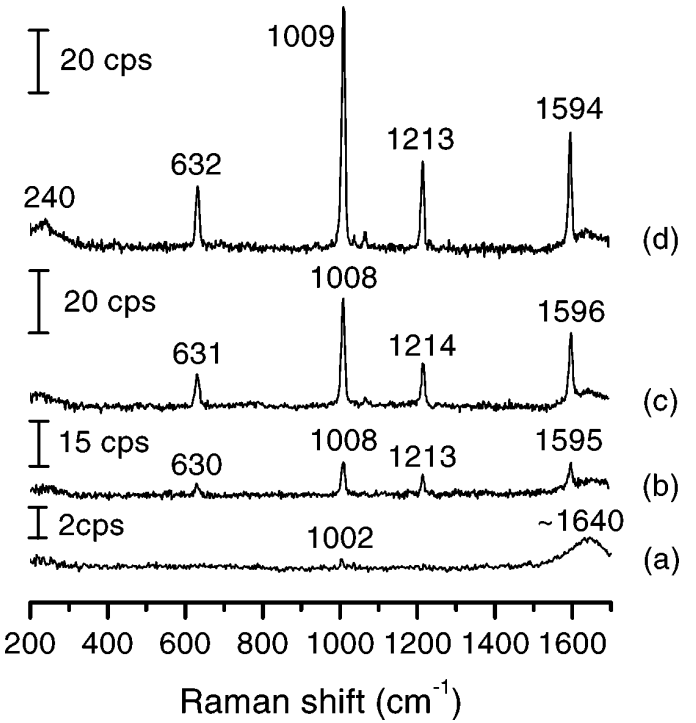

Figure 1 Surface Raman spectra of pyridine adsorbed on iron electrode surfaces prepared by different roughening procedures in a solution of 0.01 M pyridine and 0.1 M KCl: (*a*) mechanical polishing; (*b*) chemical etching in 2 M H_2SO_4; (*c*) ex situ ORC in 0.5 M H_2SO_4 by a double-step oxidation-reduction cycle (ORC) from −0.7 V to –0.35 V where the potential was held for 15 s and then returned to –0.7 V; (*d*) in situ ORC in 0.01 M pyridine +0.1 M KCl in the spectroelectrochemical cell prior to measurement. The exciting wavelength was 632.8 nm.

synthesis method on the basis of anodic aluminum oxide films one can easily find the optimum size and shape for creating maximum SERS (58, 59).

The success of obtaining SERS from transition metals is also helped greatly by precise optical coupling of the electrochemical cell and a Raman instrument. That allows one to take full advantage of high efficiency in collecting Raman light by a confocal microscope; without the accurate coupling, the surface Raman signals may not be detected at all (56). For example, the solution layer and quartz window could substantially affect the light collection efficiency of the microscope because the solid angle of the light collecting system is reduced and the image is distorted (see Figure 2). As the thickness of the solution layer is increased from about 0.2 mm to 2 mm, the Raman signal intensity decreases from 89% of the maximum intensity to 35%, respectively (see Figure 2*a*). Furthermore, as most of

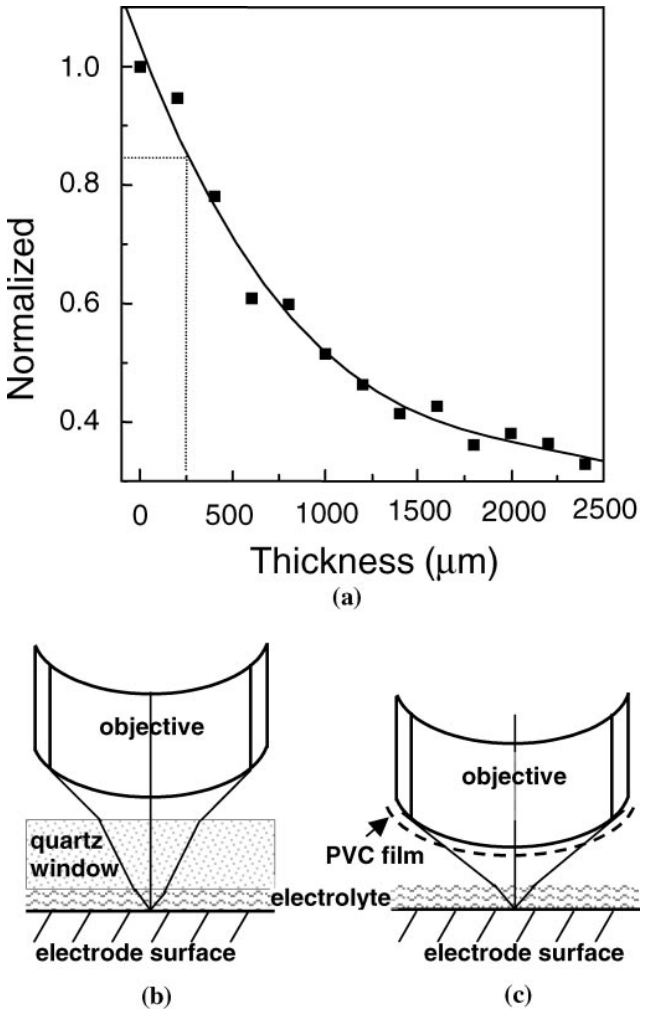

Figure 2 (*a*) The influence of the thickness of the solution overlayer between the window and the working electrode on the Raman intensity and (*b–c*) schematic diagrams of the optical configuration of a confocal Raman microscope between the sample and the objective; (*b*) with a solution layer and the spectroelectrochemical cell covered with a quartz window; (*c*) with the objective wrapped with PVC film.

the electrolytes are corrosive, a cover glass or quartz window has to be employed to protect the objective; unfortunately this results in a 50% loss of signal (see Figure 2*b*). An alternative, and the best way we found to insulate the objective, is to wrap it with a very thin and highly transparent polyvinyl chloride (PVC) film (see Figure 2*c*); with this approach, the Raman signal suffers only a 10% loss.

On the basis of the above improvements, we have been able to obtain good quality surface Raman spectra not only on electrode surfaces made from many transition metals, such as Pt, Ni, Ru, Rh, Pd, Co, Fe, and their alloys, but also over a very wide electrode potential region (e.g., –2.0 V to +1.4 V). It is particularly noteworthy that transition metals have been found to exhibit surface enhancement ranging from one to four orders of magnitude (49–60). Presently, the molecular-level investigation of diverse adsorbates at various transition metal electrodes can be realized by Raman spectroscopy (49–60). The important adsorbates already studied include CO, H, O, Cl^-, Br^-, SCN^-, CN^-, pyridine, thiourea, benzene, benzotriazole, and pyrazine (49–69). In the application section, we demonstrate the virtues of surface Raman spectroscopy for yielding information on electrochemical interfaces, e.g., those related to surface bonding, surface coverage, surface composition, coadsorbate, and electrode potential.

Improving Potential Reversibility of SERS Activity

It is a common phenomenon that the higher the SERS activity is the worse its signal stability. A typical example is that the SERS activity of an Ag electrode irreversibly decreases with time and/or applied potential, especially in the potential region where molecule desorption may occur. Taking the SERS measurement for SCN^- adsorbed on an Ag surface as an example, one can see from Figure 3*a* that the SERS intensity decreases significantly at –1.0 V from that at –0.2 V. This intensity change is not quantitatively correlated to the electrochemical data

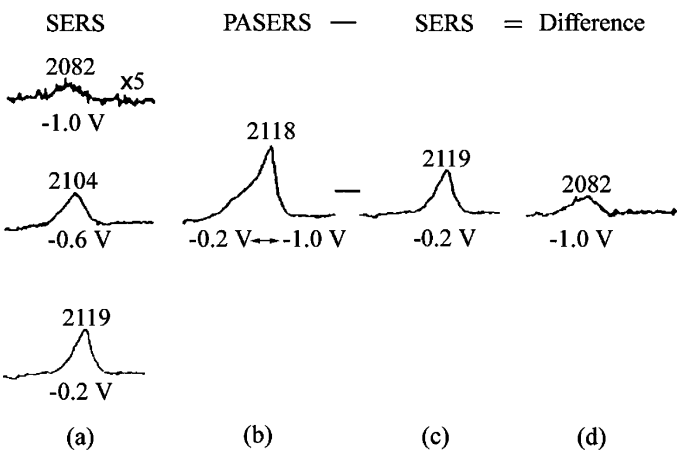

Figure 3 (*a*) SERS spectra of SCN^- adsorbed on a silver electrode at –0.2 V, –0.6 V, and –1.0 V, respectively. (*b*) PASERS spectrum of SCN^- by potential modulation between –0.2 V and –1.0 V with a modulation frequency of 10 Hz. (*c*) SERS spectrum of SCN^- at –0.2 V. (*d*) Difference SERS spectra at –1.0 V by substracting *c* from *b*. Solution is 0.1 M NaSCN + 8.0 M $NaClO_4$.

at this potential where SCN^- is only partially desorbed from the surface. This behavior has been interpreted as the decomposition followed by irreversible loss of the unstable SERS-active sites, i.e., the surface nanostructure, such as ad-atoms and ad-clusters (70). The surface-roughening procedure inevitably creates various microscopic dimensions, such as ad-atoms, ad-clusters, kinks, and vacancies as well as surface complexes. Because labile SERS-active sites need to be stabilized by an adsorbate, partial desorption of SCN^- leads to structural rearrangement and collapse of these active sites. Thus, the SERS activity does change or even is lost irreversibly upon electrochemical adsorption/desorption processes. Such changes occur unpredictably over an uneven surface, and depend on the applied voltage. Therefore, it is apparently difficult or even impossible to make a quantitative correlation of the SERS intensity with the surface coverage of the adsorbate in the entire potential region.

A unique method named potential-averaged SERS (PASERS) to overcome this problem has been successfully devised by the authors' group. This method is based on applying a continuous square wave potential modulation to the electrode during the acquisition time, as shown in Figure 4. For instance, for the acquisition

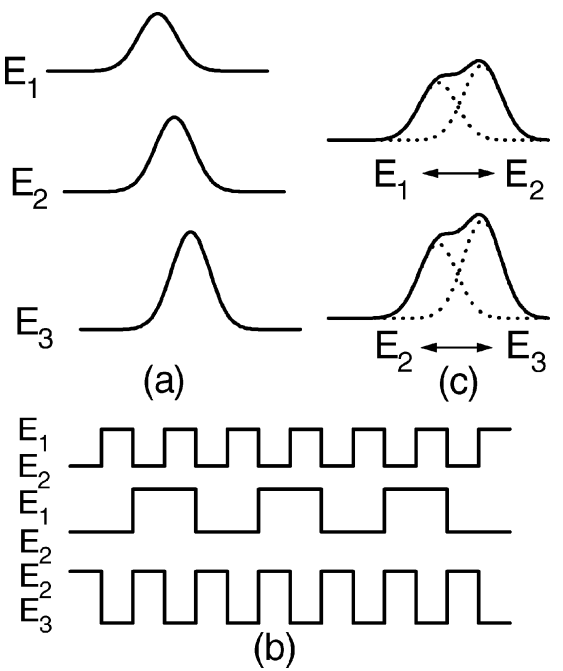

Figure 4 (*a*) The intensity and frequency of a SERS band vary with applied electrode potential. (*b*) Different voltage pulse frequencies and amplitudes can be used in PASERS measurements. (*c*) PASERS spectra at different modulating potentials, providing the sum of SERS spectra that can be detected by deconvolution.

of each data point, when a potential modulation frequency of 100 Hz and an integration time of 0.5 s are used, the potential must have been modulated 50 times during each data acquisition period. The recorded spectrum, a PASERS, is actually the superposition of the individual spectra at the two potentials being modulated. This PASERS spectrum therefore contains the spectral information of the surface species at both potentials. A set of PASERS spectra can be obtained by controlling voltage pulse amplitude or frequency, as shown in Figure 3. The essential requirement to generate such a PASERS is (*a*) to shorten the pulsing time if the applying potential resides in the SERS unfavorable region, and (*b*) to ensure the number of SERS-active sites at the two potentials being just about the same.

In the PASERS measurement of the SCN^- system, the electrode potential was modulated between –0.2 V (where SCN^- is strongly adsorbed) and –1.0 V (where it is weakly adsorbed). Because the electrode is held at the weakly adsorbed potential (at –1.0 V) for only a short time (∼0.005 s at the modulation frequency of 100 Hz, as was ∼1.0 s at –0.2 V), only a few of the most labile SERS-active sites were decomposed while most of the active sites remained structurally unchanged. Therefore, during the measurement the number of SERS-active sites at each modulated potential remained essentially the same. The upper part of Figure 3*b* is the PASERS spectrum obtained while modulating the potential between –0.2 V and –1.0 V; the shoulder at the lower frequency side is attributed to the measured SERS signal at the weak adsorption potential (–1.0 V). A deconvolution must be applied to PASERS spectra in order to gain the detailed information, and is done by choosing a modulation potential where a good normal SERS spectrum is recorded easily; in this case, it is the strong adsorption potential at –0.2 V (see Figure 3*a*). Using a suitable data manipulation process, a PASERS spectrum (Figure 3*b*) is subtracted with the appropriately chosen measured SERS spectrum at the strong adsorption potential (i.e., those of Figure 3*c*) to afford the difference spectrum that represents the "true SERS spectrum" at the other modulated potential (i.e., at –1.0 V in this case, Figure 3*d*). The "true SERS" derived from PASERS shows a considerable intensity improvement over the directly measured SERS (see the top frame of Figure 3*a* and *d*). The true SERS intensity at –1.0 V obtained by the PASERS method is about five times higher than that obtained by the directly measured SERS at comparable integration time. Therefore, by PASERS modification, the true SERS intensity with potential can be correctly correlated with the change of the surface coverage of the adsorbate, such as SCN^-, without losing considerable sensitivity even in the extreme potential region. It demonstrates that PASERS is particularly beneficial for acquiring SERS signals of adsorbates in the potential region of weak adsorption where the SERS-active sites are unstable and decompose easily.

Probing Interfacial Structure in the Potential Region of Water Electrolysis

In addition to overcoming the two limitations of SERS described above, we have also strived to take full advantage of SERS (i.e., its extremely high surface

sensitivity) to surmount some technical problems in electrochemistry. One challenging issue is how to perform measurements and extract useful information on surface electrochemical processes in the potential region involving solvent reactions. For instance, in the differential capacitance, impedance, or chronoamperometric studies, the information about surface processes of a specific species and interfacial structural changes are inevitably submerged by hydrogen evolution-induced huge Faradaic current at a high negative potential attributable to water reaction. The vast number of bubbles generated on the surface could alter the light intensity irregularly, which, in general, creates fatal interference to in situ spectroelectrochemical measurements. As a consequence, surface adsorption and reaction processes in the potential region of the solvent reactions are far from clear, in comparison to those in other potential regions, mainly owing to the lack of experimental data.

To surmount this difficulty, at least to some extent, we have tried to combine the following three approaches (62). First, to avoid the severe alternation of the incident and scattered lights by large hydrogen bubbles generated on an electrode surface, the electrode is pushed as close as possible to the cell window to form a thin-layer cell, so that the hydrogen bubbles are evolved and dispersed in very fine bubbles and escape from the thin layer smoothly. However, the compensation of ohmic drop in the thin layer should be taken into account. Second, SERS effects are utilized to dramatically increase detection sensitivity, for example to surface water. As the surface enhancement factor is 10^6, it means that the one monolayer of water molecules at the surface can be considered as equal to one million layers under normal conditions. To remove the tremendous contribution of Raman signals from the bulk water (at about 55 M in concentration) in the study of surface water, a difference spectrum method could be employed in addition to the use of a thin-layer cell. For example, a spectrum recorded at a potential that SERS effects cause to vanish completely is taken as the background and is subtracted from each measured spectrum. The remaining spectrum is important to extract the useful information, especially at potentials where SERS signals are very weak, e.g., in the extreme region (62, 71).

So far there has been much less information obtained in the potential region involving solvent reactions, such as the water electrolysis reaction. By taking the above approaches, we have successfully obtained the SERS of water in a wide potential range including in the potential region of hydrogen evolution, e.g., from –0.5 V to –2.0 V (71–73). We can perform systematic SERS studies on the effects of electrolyte ions (Li^+, Na^+, K^+, Cs^+, ClO_4^-, SO_4^{2-}, and OH^-), electrode substrates (Au, Ag, and Cu), and potentials on the SERS features of water (71–73). Figure 5 shows a set of SER spectra of H_2O and D_2O from an Au surface changing with the electrode potential. It is of special interest to find that in the potential region of hydrogen evolution, the H_2O spectral feature is strikingly different from that in the double layer potential region. The intensities of the libration and bending modes of water molecules are abnormally enhanced in comparison with that of the stretching mode (72). Based on the fact that the

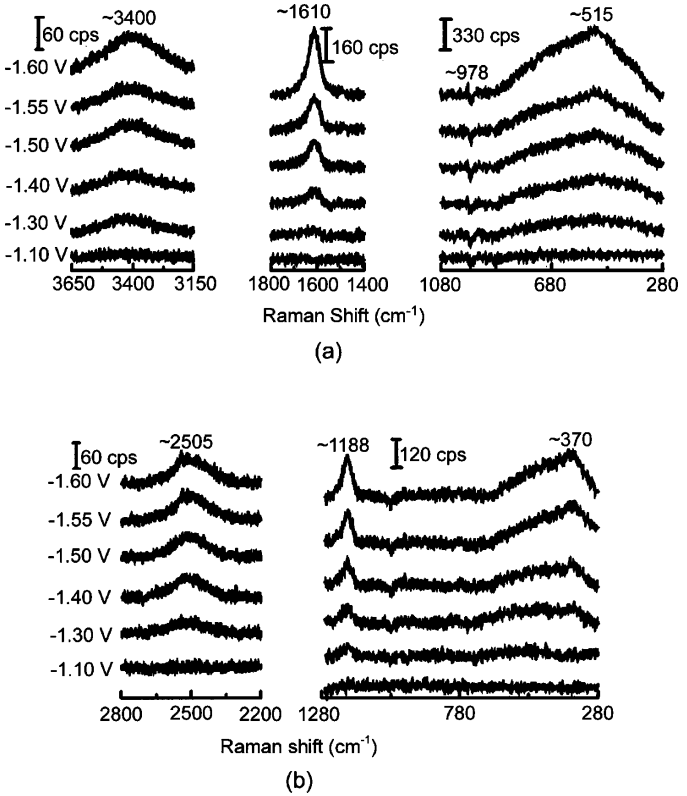

Figure 5 Surface-enhanced Raman spectra of water [(*a*) H_2O and (*b*) D_2O] from Ag in 1.0 M Na_2SO_4 at different potentials. The background spectra were recorded at –0.9 V.

strong H_2O libration band is only obtained from solid states like ice, one could assume that the interfacial water during its electrolysis process may have relatively ordered structure, enabling it to expedite electron transfer and the mobility of OH^- and H^+ through the unique hydrogen bonding network (72, 73). Although the structural information discerned from the present results is rather qualitative in nature, this preliminary study may stimulate more molecular-level research and descriptions of the interface in the potential region of solvent (water) reaction.

In summary, we are optimistic and predict that in view of the development of electrode substrates and the improvement of EC-SERS measurements, the research capability of Raman spectroscopy can be expanded and thus will lead to a powerful and general tool in electrochemistry. With the improved sensitivity provided by SERS, one can achieve high spectral resolution, reasonably good spatial

resolution, and high time resolution in the investigation of interfacial electrochemistry. Mainly on the basis of recent work from our laboratory, herein we list EC-SERS applications in electrochemical adsorption and reaction.

APPLICATIONS OF ELECTROCHEMICAL SERS

Electrochemical Adsorption

The electrochemical behavior and properties of adsorbed species play a central role in the electrode processes and in the electrocatalytic processes. SERS, with its unique high surface sensitivity and high spectral resolution, can obtain a wealth of information about electrochemical adsorption. It can easily detect and distinguish the strongly and dissociatively adsorbed species or even coadsorbed species that only weakly interact with the surface through other adsorbates.

HYDROGEN ADSORPTION Hydrogen adsorption at electrodes is one of the most important systems known in electrochemistry. It has significance in many practical systems, such as fuel cells, water electrolysis, electrochemical-sensors, and electrochemical-treatment of pollutants. The first observation of surface Raman signals of adsorbed hydrogen in electrochemical environments was reported in 1996 based on the progress mentioned in the previous section (62, 63, 74). Taking advantage of the high sensitivity and the high spectral resolution of a confocal Raman microscopy, the hydrogen adsorption at platinum electrodes has been investigated, particularly on the spectral properties influenced by the applied potential, hydrogen surface coverage, electrolyte ions, and solution pH (62, 63, 74). This seemingly simple system is by no means simple, as will be seen from the following example.

On the platinum electrode in either acidic or neutral solutions a broad band at $\sim$2088 cm^{-1}, which is assigned to vibration of the on-top adsorbed hydrogens on platinum atoms, can be observed. The dependences of the frequency, full-width at half maximum (FWHM), and intensity of this band with the electrode potential are shown in Figure 6. The FWHM decreases dramatically as the potential is moved from the hydrogen underpotential deposition (UPD) to the overpotential deposition (OPD) region (negative of –0.25 V) (see Figure 6*b*). It indicates that the nature and bonding configuration of the surface hydrogen is remarkably different in the UPD and OPD regions. The existence of different surface sites on the roughened Pt surface may lead to the difference in the local UPD and OPD potentials (63, 74). The negative movement of the potential also leads to a redshift of Pt-H vibrational frequency. This potential dependent frequency shift is difficult to understand because H atoms have no permanent dipole, and the dipole moment of Pt-H is small. Even more interestingly, the SERS intensity is substantially weaker in the UPD region, a very weak and broad band can be discernible only when the surface hydrogens are nearly saturated (63).

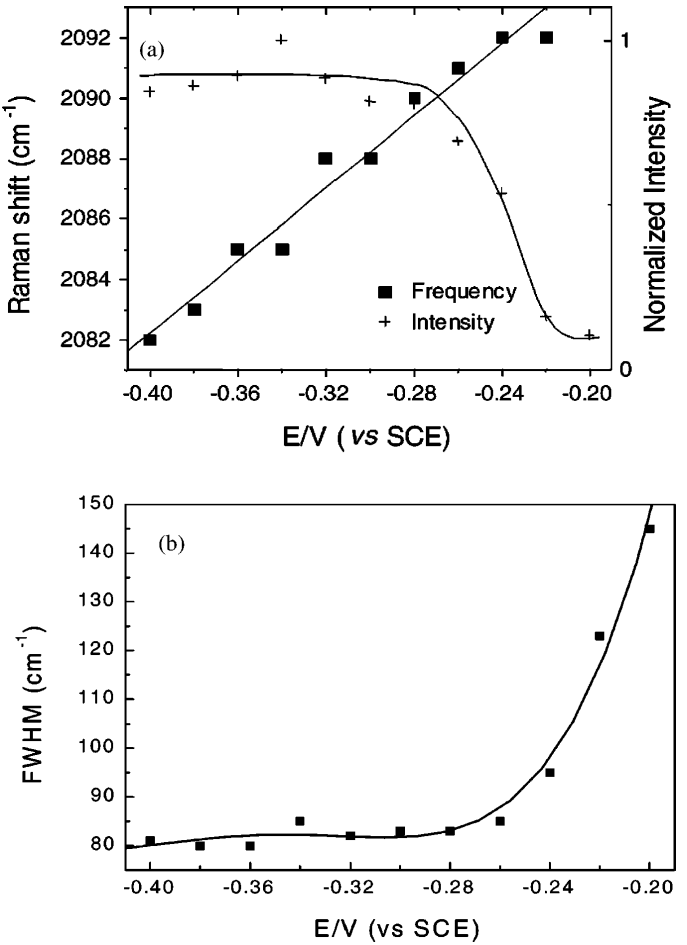

Figure 6 The dependences of the Raman shift, integrated intensity (*a*), and full-width at half maximum (*b*), with the electrode potential for the *v*(Pt-H) vibration in 0.5 M H_2SO_4 solution.

To explain the above phenomena, DFT calculations based on the cluster models have been performed (75, 76). The electrode potential effects were simulated either by charging the clusters or by considering the clusters in the presence of an unformed external field. The results showed that charging not only builds up the field, but also shifts the HOMO/LUMO levels of the clusters; and it is the shift of the work function of the substrate that leads to a large tuning rate of Pt-H frequency with the change of electrode potential. The calculations further revealed that the spectroscopic properties of Pt-H are highly sensitive to the surface coverage of

hydrogen. A redshift of Pt-H frequency with the decrease in the electrode potential would originate from the lateral interaction of Pt-H bonds. These theoretical predictions are in good agreement with the experimental observations that only when the electrode potential approaches the OPD region and only when the hydrogen adsorption reaches the monolayer can one have a detectable Pt-H vibrational intensity (62, 63).

METHANOL DISSOCIATIVE ADSORPTION With its good spectral resolution, Raman spectroscopy is also suitable for in situ monitoring of the same surface species existing in different microenvironments of the electrode/electrolyte interface. A good example is the spectral change during the dissociative adsorption and electrochemical oxidation process of methanol. Figure 7*a* shows the potential-dependent surface Raman spectra obtained on a rough Pt electrode. The frequency of the CO produced by dissociation from methanol (2045 $\sim$ 2053 cm^{-1}) is considerably lower than that adsorbed directly from solutions saturated with CO (2060 $\sim$ 2071 cm^{-1}) (77, 78). The main reason for the lower frequency is a weaker coupling between the neighboring CO (79) as a result of a lower surface coverage of CO. The lower coverage is most likely attributable to the fact that the dissociation of methanol on the Pt surface needs some additional neighboring sites around the Pt atoms.

Moreover, the CO produced by dissociation from methanol gives a wider FWHM, which may be related with kinks, edges, and steps on the roughened Pt surface. CO prefers to adsorb on these sites and its frequencies on these sites are about tens wavenumbers lower than that on the terrace. When the surface coverage is low, the adsorption state of CO on the rough surface is highly discrete leading to a wider FWHM. When the CO coverage is high, CO will still adsorb on these sites. However, the strong coupling between the CO molecules leads to a transfer of the intensity of CO from the lower frequency band to a higher frequency one (77, 79). Therefore, the vibrational state of CO on the surface will be simpler. As a result, the FWHM of CO will be much narrower.

We also found a strong influence of surface roughness on the onset potential of methanol oxidation by SERS using the platinum electrodes with different surface roughness factors ranging from 50 to 200 (61). These results have shown that Raman spectroscopy can be used more flexibly than many other spectroscopies in the study of surface bonding and highly roughened surfaces with dark color. Raman spectroscopy may provide a way to bridge the gap between the systems of fundamental research and technical applications of practical importance.

It should be pointed out that Raman spectroscopy can detect not only the CO adsorption on different surface sites, but also the influence of alien atoms on the CO frequency. When a Pt electrode was deposited with submonolayer ruthenium (Ru), which is used extensively in methanol fuel cells, the surface coverage of CO on Pt decreases leading to a lower ν_{CO}. The higher the Ru coverage, the lower the frequency of ν_{CO} and the broader the band. It is of interest that when the surface

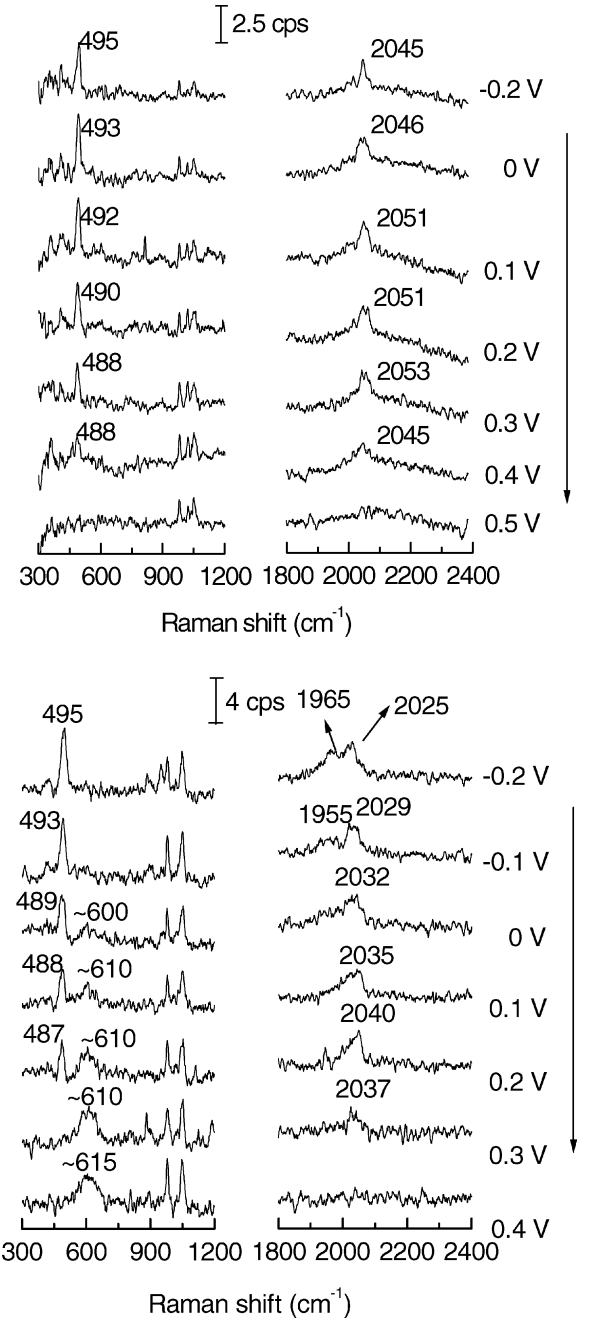

Figure 7 Surface Raman spectra from a roughened Pt electrode with roughness factor of 50 (*a*) and that covered with underpotential-deposited Ru ($\theta = 0.7$) (*b*) in 0.1 M CH_3OH + 0.1 M H_2SO_4. The excitation line: 632.8 nm.

coverage of Ru was as high as 0.7 (see Figure 7*b*), a shoulder peak appeared on the red side of the 2025 cm^{-1} peak. This peak can be reasonably assigned to the CO adsorbed onto the Ru surface. The CO/Ru peak is quite apparent in the electrode potential region more negative than –0.1 V, which can also be found in the low frequency region of the Pt– (Ru-)C bond. The low frequency band at 490 cm^{-1} is broader on the Pt-Ru surface than that on the pure Pt surface, but there is no obvious shift on the vibrational frequency in the $\nu_{Pt\text{-}C}$. In Figure 7*b*, a broad band at 600 cm^{-1} appears at 0 V and increases with the positive movement of the electrode potential, which cannot be detected under the same condition on the pure Pt electrode. Because the platinum oxides can only be observed at the potentials more positive than 0.7, it is reasonable to assign the band at 660 cm^{-1} to the oxygen-containing species on the Ru surface. The oxygen-containing species adsorbed on the Ru atom promotes the oxidation of the adjacent CO adsorbed at the Pt atom, which provides convincing evidence for the bifunctional mechanism of Ru in promoting the oxidation of methanol on the Pt surface (80). It also shows the advantage of Raman spectroscopy in directly obtaining informative spectra about surface bonding in the low frequency region.

COADSORPTION OF INORGANIC AND ORGANIC SPECIES In the above examples, the major objective is to observe molecules that have strong chemical interaction with the substrate. There are some molecules that have only very weak interaction, such as physical interaction, with the substrate. This is the common case in the coadsorption systems involving organic molecules, inorganic ions, and solvent molecules. With its high spectral resolution, SERS is very sensitive to a small change of a surface species. A careful analysis of the variation in frequency and intensity of the SERS signal of coadsorbates with the potential can yield a detailed picture of coadsorption configuration and various adsorption states (81, 82).

As a commonly used electrolyte ion, ClO_4^- does not chemically interact with Ag electrodes. No SERS signal concerning this species can be observed from the solution containing only $NaClO_4$. However, after the addition of thiourea (TU) into the solution, strong SERS signals from ClO_4^- can be detected together with that of TU, (see upper part of Figure 8). These signals indicate that the electrolyte anion is induced by the strongly adsorbed TU on the surface, as the induced coadsorption (81, 82). It is of special interest that the frequency of the coadsorbed ClO_4^- is identical to that of the free ClO_4^- and independent of the electrode potential. It implies that this anion only interacts indirectly with the surface as induced physical coadsorption. In order to analyze the detailed coadsorption configuration, we added some SO_4^{2-} into the above solution. The SERS bands from ClO_4^- were replaced completely by that from SO_4^{2-}; meanwhile the frequencies of the bands attributed to the NH_2 (3345 cm^{-1}) and the N–C–N groups (1093 cm^{-1}) of TU changed in several wavenumbers while the other bands of TU remained unchanged (83), (see lower part of Figure 8). This slight but meaningful spectral change reveals that the coadsorption of TU with electrolyte anions is through its NH_3^+ group, (see Figure 9*a*). It is necessary to point out that this kind of induced coadsorption

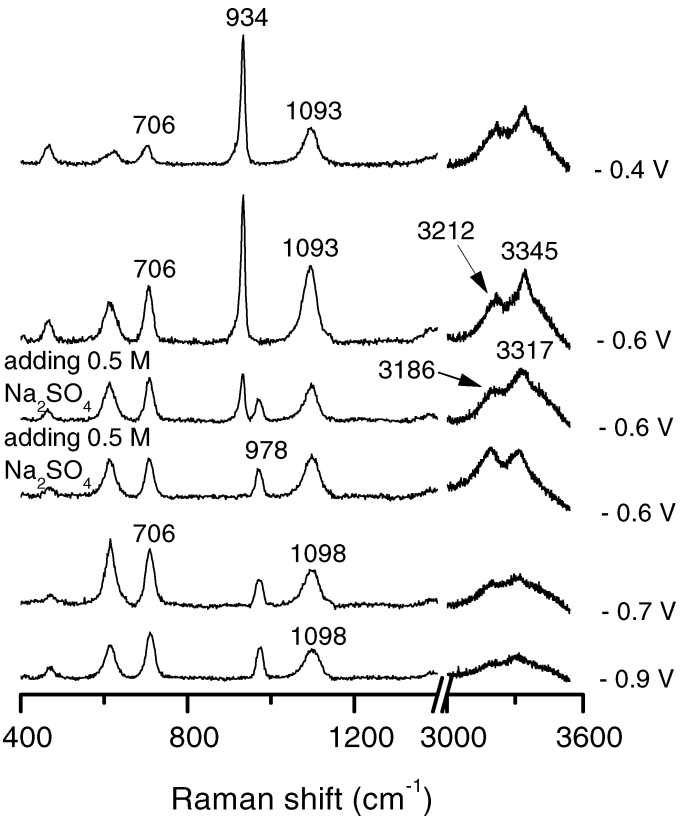

Figure 8 SERS from a Ag surface of the coadsorption process of thiourea with ClO_4^- and SO_4^{2-} as a function of the electrode potential. Excitation line: 632.8 nm.

of electrolyte ions is very difficult to detect by the conventional electrochemical methods; however, the coadsorption can be sensitively detected using SERS.

A more complicated example is the potential-dependent transition from the parallel coadsorption (competitive coadsorption) to the induced coadsorption (81). The competitive coadsorption of TU with SCN^- at relatively positive potentials can be easily understood, as two coadsorbates can interact strongly with the Ag electrode surface, as shown in Figure 9*b*. The interesting spectral feature is that the potential for observing the SERS signal of adsorbed SCN^- is more negative (e.g., –1.3 V) in comparison with the case without the presence of TU. It means that the interaction between SCN^- and TU is so strong that the anion can be induced to adsorb at relatively negative potentials where the SCN^- desorption normally takes place. Furthermore, the frequency of the C≡N band of the induced coadsorbed SCN^- was very close to that of the free SCN^-. This indicates that the

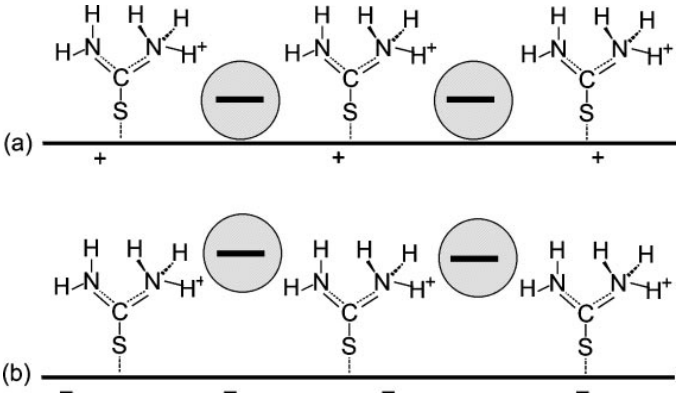

Figure 9 Adsorption model showing the coadsorption of anions (SCN^-, ClO_4^-, or SO_4^{2-}) with thiourea in the acidic solution at different potentials.

coadsorption of SCN^- and TU is transited from parallel to induced coadsorption state, as illustrated by Figure 9.

Surface Electrochemical Processes

Besides being capable of revealing the nature of the adsorption processes in static states, Raman spectroscopy can also be used to monitor the transient processes related to electrochemical adsorption and reactions at the interfaces benefiting from its high temporal and reasonably good spatial resolution.

TRANSIENT COADSORPTION PROCESS As has been seen above, the static state SERS study can provide some meaningful information, e.g., the adsorption configuration about the pertinent system. Raman spectroscopy is, in principle, amenable to the dynamic study, which affords additional information about electrochemical processes, especially the dynamic structural change. The conceptually most straightforward extensions into this field are time-resolved investigations. In the EC-SERS study, Raman signals generally can be acquired during the potential scan or after certain kinds of external stimulus. Depending on the information we are interested in, the time domain may vary from seconds to milliseconds or even to nanoseconds in an electrochemical system (83–85).

The SERS intensity change following a potential step will be slow if the surface processes are concerned with the change in the orientation of adsorbates. This usually involves the rearrangement and replacement of the surface species including solvent molecules and electrolyte ions. In contrast, the SERS intensity change with potential will be rapid if the processes only involve a mild change in the bonding strength of the adsorbate interacting with a charged surface, or are only related to the charge transfer enhancement mechanism. Therefore, a time-resolved SERS

(TRSERS) measurement, i.e., monitoring the change of SERS intensity following a potential step, can be used to make a preliminary assessment of whether a slow orientation change or a structural change in the adsorbed layer is involved for a particular system in the potential region studied.

TRSERS study of the TU + ClO_4^- coadsorption is given as the first example (83). The major SERS bands shown in Figure 8 can be divided into two groups according to their distinct intensity-time profiles. The CS stretching vibrational mode at 710 cm^{-1} and the SCNN symmetric stretching mode at 1496 cm^{-1} belong to the first group, (see Figure 10). Following the potential step, the intensity changes over 80% within the first 0.5 s, and then slowly approaches a constant value. The bands of the second group, which have a much lower changing rate of intensity, are related to vibrational modes of the amino group, at 468 cm^{-1}, 1094 cm^{-1}, and 3350 cm^{-1}, as well as those of the coadsorbed ClO_4^-. The intensity of these bands undergoes only 50% of the overall change at the initial stage of the potential step and then decreases slowly over more than 10 min. As ClO_4^- is coadsorbed on the surface by interacting with protonated amino groups, (see Figure 9*a*), both of them are not very near the surface. In order to form a well-structured coadsorbed layer at –0.3 V, the ClO_4^- ions need time to rearrange to locate at the right place. In contrast, when the potential was stepped back to a more negative potential, the

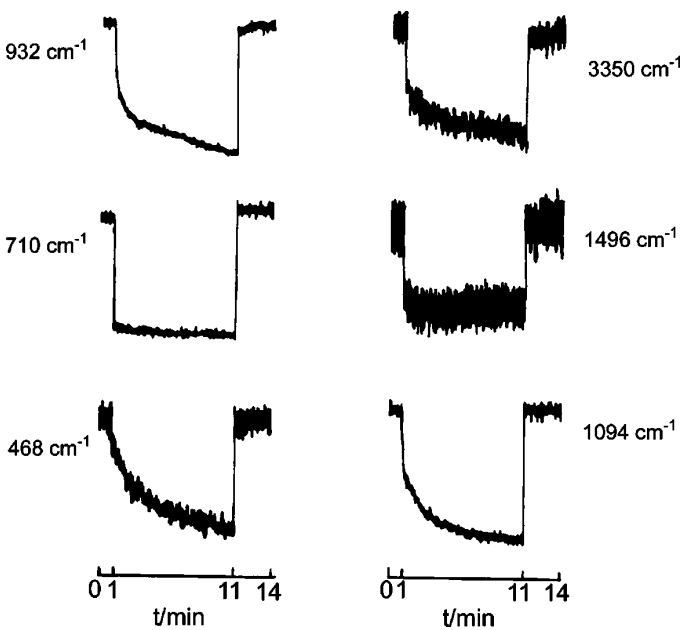

Figure 10 Dependences of the intensities for various SERS bands of TU and ClO_4^- on the double potential step. The data were manipulated by subtracting the background signal and normalized with respect to intensity.

coadsorbed layer becomes loose and disordered so that the intensity change of all the bands can follow the potential step rapidly (83).

It is necessary to point out that, in previous dynamic studies, adsorbate was considered as a whole rigid body so that the all-molecular structure will change with the potential simultaneously. The above TRSERS study reveals that the intensities of the SERS bands arising from different vibrational modes (i.e., different groups) of an adsorbate can have different response rates to a potential change. By taking advantage of combining spectral and time resolution, one is able to focus on individual bonds of the adsorbate in surface dynamic studies, particularly in some complicated coadsorption processes (83).

TRANSIENT REDUCTION PROCESS In an electrochemical reaction, the reaction rate is normally much higher than that of the coadsorption process. With a fast optical multichannel analyzer (such as PDA), it is possible to obtain the SERS of surface reactions during a potential ramp, which is extremely important when irreversible processes occur. This kind of process normally occurs at a scale of milliseconds. A good example is the combined SERS and cyclic voltammetric study of nitrobenzene surface reactions on a SERS-active Au surface, reported by Gao et al. (84). It is known that nitrobenzene can be reduced to nitrosobenzene, phenylhydroxylamine, and aniline through three two-electron steps:

$$C_6H_5NO_2 \xrightarrow{2e^-} [C_6H_5NO] \xrightarrow{2e^-} C_6H_5NHOH \xrightarrow{2e^-} C_6H_5NH_2$$

Nitrosobenzene was not detected by analytical methods, and it is possible that it is consumed by a chemical coupling reaction following the electrochemical reaction:

$$C_6H_5NO + C_6H_5NHOH \longrightarrow C_6H_5N = N(O)C_6H_5$$

From the cyclic voltammograms of nitrobenzene in sulfuric acid solution in Figure 11*a*, one can find a pair of peaks at –0.11 and –0.27 V of the reduction of nitrobenzene. The anodic peak at 0.33 V has been assigned to the formation of nitrosobenzene, and the cathodic peak at 0.30 V is from the reduction of nitrosobenzene to phenylhydroxylamine. The 30 mV separation, independent of the scan rate, indicates that the above pair of reactions present a reversible process. The SER spectra were acquired during the potential sweep for the reduction of nitrobenzene at a gold electrode, (see Figure 11*b*). It can be seen during the positive movement of the electrode potential, the band at 1330 cm^{-1} corresponding to the nitrobenzene decreases. Meanwhile, new bands located at 1146, 1388, and 1588 cm^{-1}, respectively, appear when the potential is negative of –0.11 V. Compared with the normal Raman and SER spectra of possible reaction products, these new peaks are essentially the features of nitrosobenzene. Correlating the voltammetric and SERS results, the peak at –0.11 V in the cyclic voltammogram can be assigned to the reduction of nitrobenzene to nitrosobenzene (84). This study provides a good example of the combination of electrochemical methods and SERS to investigate the pathways and intermediates of electrochemical reactions.

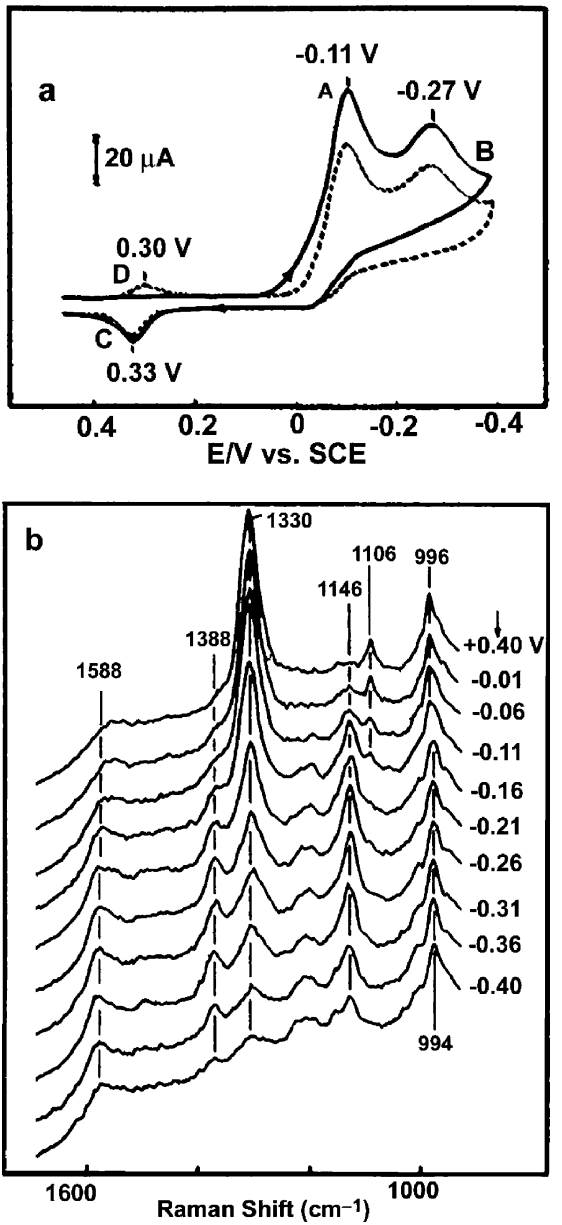

Figure 11 (*a*) Cyclic voltammograms for 1 mM nitrobenzene in 0.1 M H_2SO_4 at a gold electrode. Solid and dashed traces refer to first and second consecutive cycles, respectively. Scan rate: 100 mV/s. (*b*) Sequence of surface-enhanced Raman spectra obtained during the reduction of nitrobenzene at the gold electrode. Scan rate: 5 mV/s, negative—going from 0.4 V versus SCE. Solution: 3×10^{-3} M nitrobenzene +0.1 M H_2SO_4. Excitation line: 647.1 nm. (Reproduced with permission from Reference 84. Copyright 1988, American Chemical Society.)

FAST PHOTOCHEMICAL PROCESS Pump and probe techniques in principle can reach time resolution as high as that provided by the laser pulse that ranges from nanoseconds to femtoseconds. It is performed at steady state of a surface process that can be disturbed by a pump pulse laser and probed by another CW laser, which is suitable to probe surface charge transfer processes and characterize vibrational energy transfer rates for surface species (85). The probe laser is illuminated on the sample during the whole measurement. The higher the time resolution value required, the stronger the Raman signal should be. Thus, in the nanosecond-resolved Raman studies, a molecule with very strong resonance and/or surface-enhanced Raman effects is adopted in order to provide a strong-enough signal.

Zhang et al. (86) reported a nanosecond time-resolved Raman study on the photochemical process of flavin mononucleotide (FMN) at a silver electrode. Figure 12*a* gives the Raman spectrum before the pumping of the UV laser, showing the characteristic band of FMN. After photoinitiation for 75 ns, the bands at 1092

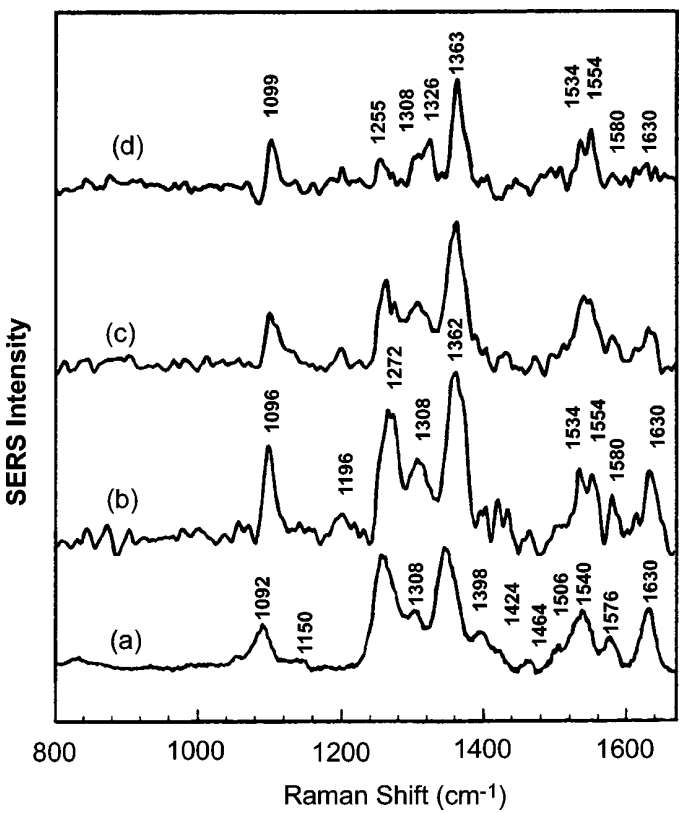

Figure 12 Time-resolved SERS spectra of flavin mononucleotide as a function of delay time with 337 nm pulsed excitation and 488 nm CW probe laser light. Acquisition time: 200 ns. Delay time: (*a*) 0 ns; (*b*) 75 ns; (*c*) 375 ns; (*d*) 775 ns. (Reproduced with permission from Reference 86. Copyright 1995, American Chemical Society.)

and 1348 cm^{-1}, 1260 cm^{-1} and 1398, and 1424 cm^{-1} blueshift (see Figure 12*b*). They are assigned to ring II, ring III, and N_3–H vibrations, respectively. A new band at 1196 cm^{-1} appears, which is related to the mixed C–O–H bending and stretching. It indicates that a proton transfer is taking place from N_3–H to the adjacent carbonyl to form a new C–O–H bond within 75 ns. However, it disappears at 775 ns (see Figure 12*d*), instead a band at 1326 cm^{-1} appears, which is related to the ring III secondary-amine stretching mode. Meanwhile the band at 1272 cm^{-1} (ring III stretching mode) redshifts to 1255 cm^{-1}, and the band at 1096 cm^{-1} (ring II stretching mode) blueshifts to 1099 cm^{-1}. However, other ring II and III stretching modes remain unchanged at times longer than 775 ns. Therefore, at this time domain, ring III loses some bond order or aromaticity. Based on this TRSERS study, the authors proposed a possible reaction process that is shown in Scheme I (86). With this pump and probe technique, it is very promising to monitor the whole charge transfer process of an electrode surface species or a surface metal complex.

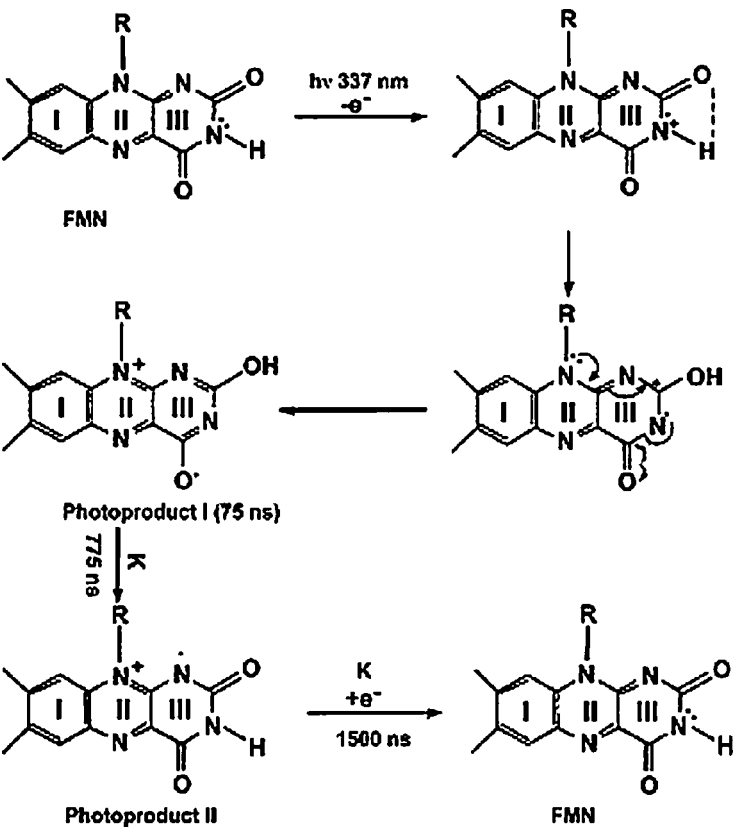

Scheme I The overall photoinduced kinetic process of flavin mononucleotide. (Reproduced with permission from Reference 86. Copyright 1995, American Chemical Society.)

LOCALIZED ELECTRODE REACTION Besides the ability of identifying the adsorption and reaction behavior of surface species as well as providing detailed information on some dynamic processes occurring at/in the electrochemical interfaces, Raman spectroscopy can still provide additional information for surface studies with its reasonably good spatial resolution at the micrometer scale.

In corrosion science, the most frequently met surfaces are heterogeneous either in morphology or chemical composition. As a result of the heterogeneity, the surface reactions may be different in different areas of the surface resulting in pitting corrosion, the latter magnifying the heterogeneity. With its good two-dimensional resolution, confocal Raman microscopy can provide quite high resolution determined by the size of a laser spot and the stepping resolution of an X-Y scanning stage. A resolution of $1 \sim 2$ μm is sufficient to study a nonuniform surface such as a corrosion pit in a rebar electrode (87). A pit was found with the optical microscope, (see Figure 13*a*) and the Raman spectrum (not given) obtained in the pit reveals that it contains several corrosion products, including γ-Fe_2O_3, Fe_3O_4 (550 cm^{-1}), γ-FeOOH, and Cl^--containing iron compound (324 cm^{-1}). Then the bands of different corrosive products, e.g., Fe_3O_4 and Cl^--containing iron compounds, were selected as the signaling bands. After that, the laser spot was scanned across the pit and the Raman signal of selected bands was recorded with the change of the position, given in Figure 13*b* and *c*. It is interesting to find that along the scanning line the two species show different intensities at different positions indicating a clear spatial variation of the composition and electronic properties of the passive film across the pit region on metal electrodes. The two-dimensional Raman images of different corrosive products can also be obtained but the acquisition procedure is rather time consuming.

Microprobe Raman spectroscopy can be also employed to study some microscopic processes occurring at an electrode surface during an electrochemical reaction. The cyclic voltammetric study of benzene on a Pt electrode in 0.1 M $HClO_4$ did not provide more information than showing a broad oxidation peak. However, a Raman study on the surface revealed an amazing phenomenon when a very negative or positive potential was applied to the Pt electrode (88, 89). In both cases, very evenly distributed liquid drops were observed on the electrode surface on the microscopic TV monitor equipped with the microprobe Raman system and grew gradually either with the prolonging time or further negative- or positive-shift of the potential, indicating the occurrence of a certain kind of surface reactions. Figures 14*a* and *b* show a typical surface morphology of a smooth Pt electrode covered with drops at –0.325 V and 1.2 V. With the Raman microscope, one can easily focus the laser into the drops and the gaps among them. The signal from the gap shows the same feature as the bulk solution. However, the Raman feature of surface drops is obviously different from that from the gap, shown in Figure 14*c*. Except for a 990 cm^{-1} band from the ring breathing mode of benzene and a 933 cm^{-1} band from the supporting electrolyte (ClO_4^-), all other bands present the features of cyclohexane and chlorobenzene. Therefore, at negative potentials ($<$–0.325 V), benzene can be reduced to cyclohexane (see lower spectrum

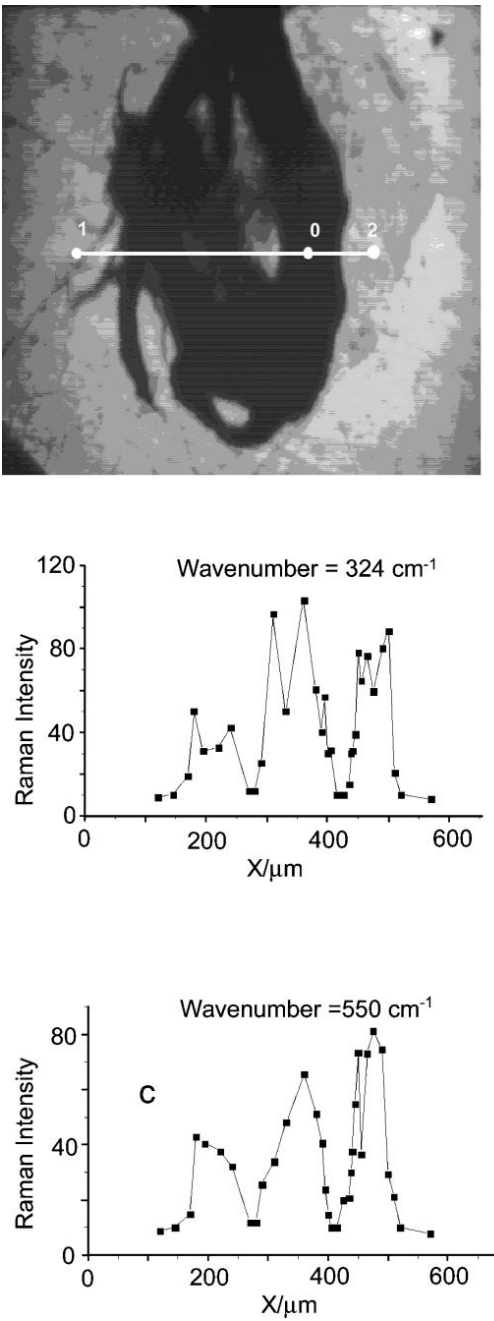

Figure 13 The TV image of the rebar electrode after it was corroded (*a*), and the surface Raman profiles for the selected bands at 324 cm^{-1} (*b*) and 550 cm^{-1} (*c*) upon the line 1–2.

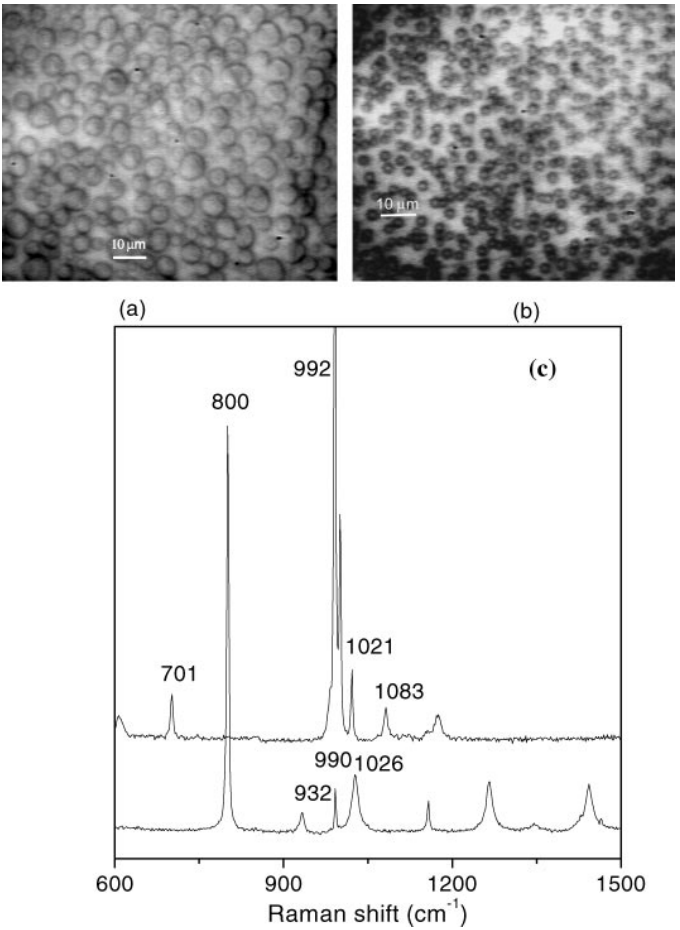

Figure 14 TV images of surface drops formed during the reduction process in 6 mM benzene +0.1 M $HClO_4$ (*a*) and chlorination process in oversaturated benzene +0.1 M KCl (*b*) and the corresponding Raman spectra from the surface drops (*c*).

in Figure 14*c*), while at positive potentials (>1.2 V) it can be chlorized into chlorobenzene (see upper spectrum in Figure 14*c*). Because both products are insoluble in water, they form drops adhering on the electrode surface. As benzene has a higher solubility in cyclohexane and chlorobenzene than in water, it can be extracted from water to the surface drops. This resulted in a fast decrease in the Raman intensity of benzene in the aqueous solution phase and a strong signal of benzene in the surface drops. The reduction and chlorination processes of benzene are both influenced significantly by the roughness of the electrode surface. Both processes occur more easily on a rough surface than on a smooth surface. In the Br^- solution, the halogenation process takes place more vigorously. No fluorination

and iodination occurs in F^- and I^- solution, owing to the high stability of F^- and active chemical property of I_2 (89). This study shows that Raman microscopy is very helpful for identifying surface reaction products microscopically and postulating the surface reaction mechanism.

OUTLOOK AND SUMMARY

Along with significant developments in nanoscience, many opportunities have provided and will continue to provide for fundamental progress in SERS to further enhance its capability for studying electrochemical interfaces. Recently, a breakthrough has been made in the SERS field. Enormous enhancements of up to 14 orders of magnitude have been achieved so that high-quality SERS or surface-enhanced resonance Raman scattering (SERRS) spectra from a single molecule adsorbed on the surface of single silver or gold particles or aggregated colloids have been obtained (90–93). It is of particular interest that substrates with particle sizes of about 90 nm for Ag and about 60 nm for Au present the highest enhancement effect (94). In comparison with the normal enhancement of six orders of magnitude, this phenomenon indicates that SERS substrates with much higher activity can be prepared, in particular with the aid of nanofabrication technology (95–97). Many electrode substrates with higher SERS activity may be made, and the detection sensitivity of SERS for a variety of electrode materials including transition metals will be further improved.

For three noble metals (Au, Ag, and Cu), the excitation lines have only covered the visible spectrum up to the near-infrared region, from 450 nm to 1064 nm. There are inherent difficulties in using the ultraviolet excitation that could explain the absence of these data in the SERS literature. Electromagnetic enhancements are rather small in the ultraviolet region where damping is generally large due to interband transitions. Since the optical property of transition metal is different from that of the noble metals, it is worth testing these new systems. Very recently we reported the first UV-SERS spectra of molecules adsorbed onto rough rhodium (Rh) and ruthenium (Ru) metal surfaces (98). Hopefully, this new trend will be facilitated by the fast development of commercial low cost UV laser and UV-Raman systems. UV-SERS will be further applied in fields that include electrochemistry, biomedicine and catalysis as well as theoretical investigation counting SERS itself.

One of the remaining technical challenges is how to extend the SERS substrate from the rough and nanostructured surface to the atomically flat single-crystal surface. A SERS study using an ATR Raman cell with the Otto configuration on a truly smooth single crystal surface under electrochemical conditions was reported recently (99). The enhancement factor, assisted by the surface plasma enhancement, for a single crystal Cu surface is estimated to be around one to two orders. There have been only a very limited number of molecules with large Raman cross sections studied using this rather complex configuration. The major technical improvement for ATR-SERS seems to be required in order to make it widely used. Very recently, tip-enhanced Raman spectroscopy has been developed, which

combines Raman spectroscopy with an STM tip (100, 101) or metal-coated AFM tip (102–105) used as an amplifier of the electromagnetic field at smooth surfaces. The field enhancement by the tip is attributable to the excitation of localized surface plasmons, which is also effective in the substrate areas in close proximity to the tip apex. Thus, the illuminated tip in working mode can induce the SERS of adsorbates at the smooth surfaces of any materials. Although this new technique has not yet been applied to electrode surfaces and single crystal surfaces, it shows a very promising future for two reasons: it can study atomic flat surfaces and has a very high spatial resolution.

In spite of the fact that the Raman frequency shifts of the adsorbate on metal surfaces have been investigated extensively (28–32, 55, 60), the systematic study on the relative band intensity of various bands for the adsorbate is very limited (10, 28). A quantitative explanation for the relative intensity differences at different potentials or on different metal surfaces is still substantially lacking. It should be pointed out that people have not been able to use the SERS mechanism (29, 30) to well interpret the origin of the different relative intensity, even for the most typical pyridine/electrode system. Thus, it seems to be worthwhile to pay strong attention to the relative band intensity from a more fundamental point of view, i.e., through the quantum chemical calculation to spectral intensities of various vibrational modes to reveal the complex surface-molecule interaction (106–108). This theoretical approach combined with the study of SERS mechanism could be important for the further development of the EC-SERS technique.

The ultimate goal for establishing EC-SERS as a standard technique must rely on complete understanding of SERS mechanisms (29–32, 55). The photon-driven charge transfer (CT) enhancement is much more complicated than the electromagnetic enhancement. The former could be considered as a resonance-like Raman enhancement. The intermediate state of the Raman process is the CT state associated with the charge transfer between the molecule and the metal surface (10, 30–32). This mechanism can be clearly verified by obtaining the intensity-potential profile with the changing exciting line (the incident photon energy) (10, 28). The involvement of the CT mechanism generally makes the analysis of SERS spectra and theoretical interpretation more difficult and complicated. However, in our opinion, this disadvantage may be turned into an advantage for EC-SERS. It means that EC-SERS may be applied as a new means to probe the energetic levels of the adsorbate or the surface complex acting as the SERS-active site (73). One can use the tunable laser to tune the incident photon energy and/or move the applied potential to tune the Fermi level in order to match the specific CT state. By analyzing these SERS intensity-potential profiles of the probe molecules with different excitations, one may probe the surface state of some nanostructures, the new energy level of surface complexes upon adsorption, or the intermediate energy levels of surface species generated during electrochemical reaction processes.

In summary, through about three decades of research effort by many groups including ours, EC-SERS has been developed continually in order to fully exploit its strengths and offset the shortcomings as applied in surface electrochemistry.

The various surface roughening procedures for different electrodes and the use of a highly sensitive confocal microprobe Raman system enable us to obtain good-quality SER spectra of organic and inorganic molecules adsorbed at roughened Pt, Ni, Co, Fe, Pd, Rh, Ru, and their alloy electrodes over a wide applied potential range. Successful applications in electrochemical adsorption, electrocatalysis, and corrosion demonstrate that SERS can be widely used to investigate diverse molecules as well as substrates that were commonly considered to be non-SERS active. This exciting progress has led us to believe that a revitalization of broad interest in EC-SERS is imminent. It will offer intriguing opportunities for the molecular-level investigation of surface (interfacial) electrochemical processes.

ACKNOWLEDGMENTS

This work has been made possible by the continuous financial support of the Natural Science Foundation of China and the Ministry of Education of China under contracts Nos. 20021002, 20228020, and 90206039. Whenever the work from the authors' group is mentioned, we are grateful for the contribution of the self-motivated and hard-working students and all other group members. The authors are very grateful to Prof. Y.L. Chow for careful editing of the English.

The *Annual Review of Physical Chemistry* is online at http://physchem.annualreviews.org

LITERATURE CITED

1. Lipkowski J, Ross PN, eds. 1992. *Adsorption at Electrode Surface*. New York: VCH. 426 pp.
2. Schmickler W, Parsons R. 1997. *Interfacial Electrochemistry.* London: Oxford Univ. Press. 304 pp.
3. Bard AJ, Faulkner LR. 2000. *Electrochemical Methods: Fundamentals and Applications*. New York: Wiley. 833 pp. 2nd ed.
4. White RE, Bockris JO'M, Conway BE, Yeager E, eds. 1984. *Comprehensive Treatise of Electrochemistry*,Vol. 8. New York: Kluwer. 620 pp.
5. Abruna HD, ed. 1991. In *Electrochemical Interfaces—Modern Techniques for in-situ Interface Characterization*. Berlin: VCH Verlag Chem. 587 pp.
6. Wieckowski A, ed. 1999. *Interfacial Electrochemistry*. New York: Marcel Dekker. 996 pp.
7. Bewick A, Pons S. 1985. In *Advances in Infrared and Raman Spectroscopy*, ed. RJH Clark, RE Hester, 12:1–63. Chichester, UK: Wiley
8. Iwasita T, Nart FC. 1997. *Prog. Surf. Sci.* 55:271–340
9. Fleischmann M, Hill IR. 1984. See Ref. 4, pp. 373–432
10. Birke RL, Lu T, Lombardi JR. 1991. In *Techniques for Characterization of Electrodes and Electrochemical Processes*, ed. R Varma, JR Selman, pp. 211–77. New York: Wiley
11. Pettinger B. 1992. See Ref. 1, pp. 285–345
12. Tadjeddine A, Le Rille A. 1999. See Ref. 6, pp. 317–43
13. Williams CT, Beattie DA. 2002. *Surf. Sci.* 500:545–76
14. Pettinger B, Bilger C, Lipkowski J, Schmickler W. 1999. See Ref. 6, pp. 373–404

15. Kolb DM. 1988. In *Spectroelectrochemistry: Theory and Practice*, ed. RJ Gale, pp. 87–188. New York: Plenum
16. Abruna HD. 1991. See Ref. 5, pp. 1–54
17. Kolb DM. 2001. *Angew. Chem. Int. Ed.* 40:1162–81
18. Magnussen OM. 2002. *Chem. Rev.* 102:679–725
19. Hillman AR, Saville PM, Glidle A, Richardson RM, Roser SJ, Swann MJ, Webster JRP. 1998. *J. Am. Chem. Soc.* 120:12882–90
20. Burgess I, Zamlynny V, Szymanski G, Schwan AL, Faragher RJ, Lipkowski J, Majewski J, Satija S. 2003. *J. Electroanal. Chem.* 550:187–99
21. Lipkowski J, Schmickler W, Kolb DM, Parsons R. 1998. *J. Electroanal. Chem.* 452:193–97
22. Lipkowski J, Stolberg L. 1992. See Ref. 1, pp. 171–238
23. Ross PN, Lipkowski J, eds. 1993. *Structure of Electrified Interfaces.* New York: Wiley. 406 pp.
24. Fleischmann M, Hendra PJ, McQuillan AJ. 1973. *J. Chem. Soc.-Chem. Commun.* pp. 80–81
25. Jeanmaire DL, Suchanski MR, Van Duyne RP. 1975. *J. Am. Chem. Soc.* 97:1699–707
26. Fleischmann M, Hendra PJ, McQuillan AJ. 1974. *Chem. Phys. Lett.* 26:163–66
27. Jeanmaire DJ, Van Duyne RP. 1977. *J. Electroanal. Chem.* 84:1–20
28. Van Duyne RP. 1979. In *Chemical Biochemical Applications of Lasers*, ed. CB Moore, 4:101–85. New York: Academic
29. (a) Moskovits M. 1985. *Rev. Mod. Phys.* 57:783–826; (b) Moskovits M, Tay LL, Yang J, Haslett T. 2002. *Top. Appl. Phys.* 82:215–27
30. (a) Otto A, Mrozek I, Grabhorn H, Akemann W. 1992. *J. Phys. Condens. Matter* 4:1143–212; (b) Otto A. 2003. *Indian J. Phys.* 77B:63–73
31. Campion A, Kambhampati P. 1998. *Chem. Soc. Rev.* 27:241–50
32. Chang RK, Furtak TE, eds. 1982. *Surface Enhanced Raman Scattering*, New York: Plenum. 423 pp.
33. Cooney RP, Fleischmann M, Hendra PJ. 1977. *J. Chem. Soc. Chem. Commun.*, pp. 235–37
34. Yamada H, Yamamoto Y. 1983. *Surf. Sci.* 134:71–90
35. Bilmes SA, Rubim JC, Otto A, Arvia AJ. 1989. *Chem. Phys. Lett.* 159:89–96
36. Taylor CE, Pemberton JE, Goodman GG, Schoenfisch MH. 1999. *Appl. Spectrosc.* 53:1212–21
37. Leung LWH, Weaver MJ. 1987. *J Electroanal. Chem.* 217:367–84
38. Fleischmann M, Tian ZQ, Li LJ. 1987. *J. Electroanal. Chem.* 217:397–410
39. Van Duyne RP, Haushalter JP. 1983. *J. Phys. Chem.* 87:2999–3003
40. Oblonsky LJ, Devine TM, Ager JW, Perry SS, Mao XL, Russo RE. 1994. *J. Electrochem. Soc.* 141:3312–17
41. Zou SZ, Williams CT, Chen EKY, Weaver MJ. 1998. *J. Am. Chem. Soc.* 120:3811–12
42. Zou SZ, Williams CT, Chen EKY, Weaver MJ. 1998. *J. Phys. Chem. B* 102:9039–49
43. Zou SZ, Weaver MJ. 1998. *Anal. Chem.* 70:2387–95
44. Williams CT, Takoudis CG, Weaver MJ. 1998. *J. Phys. Chem. B* 102:406–16
45. Luo H, Weaver MJ. 1999. *Langmuir* 15:8743–49
46. Zou SZ, Weaver MJ, Li XQ, Ren B, Tian ZQ. 1999. *J. Phys. Chem. B* 103:4218–22
47. Weaver MJ, Zou SZ, Chan HYH. 2000. *Anal. Chem.* 72:A38–47
48. Park S, Yang PX, Corredor P, Weaver MJ. 2002. *J. Am. Chem. Soc.* 124:2428–29
49. Tian ZQ, Ren B, Mao BW. 1997. *J. Phys. Chem. B* 101:1338–46
50. Huang QJ, Yao JL, Gu RA, Tian ZQ. 1997. *Chem. Phys. Lett.* 271:101–6
51. Cao PG, Yao JL, Ren B, Mao BW, Gu RA, Tian ZQ. 2000. *Chem. Phys. Lett.* 316:1–5
52. Gao JS, Tian ZQ. 1997. *Spectrochim. Acta A* 53:1595–1600
53. Wu DY, Xie Y, Ren B, Yan JW, Mao BW, Tian ZQ. 2001. *Phys. Chem. Commun.* 18:U1–3

54. Cai WB, Ren B, Li XQ, She CX, Liu FM, et al. 1998. *Surf. Sci.* 406:9–22
55. Tian ZQ, Ren B, Wu DY. 2002. *J. Phys. Chem. B* 106:9463–83
56. Ren B, Lin XF, Jiang YX, Cao PG, Xie Y, et al. 2003. *Appl. Spectrosc.* 57:419–27
57. Ren B, Lin XF, Yan JW, Mao BW, Tian ZQ. 2003. *J. Phys. Chem. B* 107:899–902
58. Yao JL, Tang J, Wu DY, Sun DM, Xue KH, et al. 2002. *Surf. Sci.* 514:108–16
59. Yao JL, Pan GP, Xue KH, Wu DY, Ren B, et al. 2000. *Pure Appl. Chem.* 72:221–28
60. Tian ZQ, Gao JS, Li XQ, Ren B, Huang QJ, et al. 1998. *J. Raman Spectrosc.* 29:703–11
61. Ren B, Li XQ, She CX, Wu DY, Tian ZQ. 2000. *Electrochim. Acta* 46:193–205
62. Tian ZQ, Ren B, Chen YX, Zou SZ, Mao BW. 1996. *J. Chem. Soc. Faraday Trans.* 92:3829–38
63. Ren B, Xu X, Li XQ, Cai WB, Tian ZQ. 1999. *Surf. Sci.* 427/428:157–61
64. Ren B, Huang QJ, Xie Y, Tian ZQ. 2000. *Anal. Sci.* 16:225–30
65. Tian ZQ, Ren B. 2000. In *Encyclopedia of Analytic Chemistry*, ed. RA Meyers, pp. 9162–201. Chichester, UK: Wiley
66. Cao PG, Yao JL, Ren B, Gu RA, Tian ZQ. 2002. *J. Phys. Chem. B* 106:7283–85
67. Ren B, Wu DY, Mao BW, Tian ZQ. 2003. *J. Phys. Chem. B* 107:2752–58
68. Ren B, Cui L, Lin XF, Tian ZQ. 2003. *Chem. Phys. Lett.* 376:130–35
69. Cao PG, Yao JL, Zheng JW, Gu RA, Tian ZQ. 2002. *Langmuir* 18:100–4
70. Tian ZQ, Li WH, Mao BW, Zou SZ, Gao JS. 1996. *Appl. Spectrosc.* 50:1569–77
71. Zou SZ, Chen YX, Mao BW, Ren B, Tian ZQ. 1997. *J. Electroanal. Chem.* 424:19–24
72. Chen YX, Tian ZQ. 1997. *Chem. Phys. Lett.* 281:379–83
73. Chen YX, Zou SZ, Huang KQ, Tian ZQ. 1998. *J. Raman Spectrosc.* 29:749–56
74. Ren B, Huang QJ, Cai WB, Mao BW, Liu FM, Tian ZQ. 1996. *J. Electroanal. Chem.* 415:175–78
75. Xu X, Ren B, Wu DY, Xian H, Lu X, et al. 1999. *Surf. Interf. Anal.* 28:111–14
76. Xu X, Wu DY, Ren B, Xian H, Tian ZQ. 1999. *Chem. Phys. Lett.* 311:193–201
77. Weaver MJ, Zou S. 1998. In *Spectroscopy for Surface Sciences*, ed. RJH Clark, RE Hester, pp. 219–72. Chichester, UK: Wiley
78. Korzenkniewski C. 1999. See Ref. 6, pp. 345–52
79. Browne VM, Fox SG, Hollins P. 1991. *Catal. Today* 9:1–14
80. She CX, Xiang J, Ren B, Zhong QL, Wang XC, Tian ZQ. 2002. *J. Kor. Electrochem. Soc.* 5:221–25
81. Tian ZQ, Li WH, Qiao ZH, Lin WF, Tian ZW. 1995. *Russ. J. Electrochem.* 31:935–40
82. Tian ZQ, Ren B. 2000. *Chin. J. Chem.* 18:135–46
83. Tian ZQ, Li WH, Mao BW, Gao JS. 1994. *J. Electroanal. Chem.* 379:271–79
84. Gao P, Gosztola D, Weaver MJ. 1988. *J. Phys. Chem.* 92:7122–30
85. Birke RL, Lombardi JR. 1994. *Mol. Eng.* 4:277–310
86. Zhang W, Vivoni A, Lombardi JR, Birke RL. 1995. *J. Phys. Chem.* 99:12846–57
87. Ren B, Yao JL, Li XQ, Chen XG, Liu FM, et al. 1998. *Proc. Int. Conf. Raman Spectrosc., 16th, Cape Town*, pp. 808–9. New York: Wiley
88. Liu GK, Yao JL, Ren B, Gu RA, Tian ZQ. 2002. *Electrochem. Commun.* 4:392–96
89. Liu GK, Ren B, Gu RA, Tian ZQ. 2002. *Chem. Phys. Lett.* 364:593–98
90. Kneipp K, Wang Y, Kneipp H, Perelman LT, Itzkan I, et al. 1997. *Phys. Rev. Lett.* 78:1667–70
91. Nie S, Emory SR. 1997. *Science* 275:1102–6
92. Xu HX, Bjerneld EJ, Kall M, Borjesson L. 1999. *Phys. Rev. Lett.* 83:4357–60
93. Michaels AM, Nirmal M, Brus LE. 1999. *J. Am. Chem. Soc.* 121:9932–39

94. Krug JT, Wang GD, Emory SR, Nie S. 1999. *J. Am. Chem. Soc.* 121:9208–14
95. Dick LA, McFarland AD, Haynes CL, Van Duyne RP. 2002. *J. Phys. Chem. B* 106:853–60
96. Haynes CL, Van Duyne RP. 2001. *J. Phys. Chem. B* 105:5599–611
97. Routkevitch D, Haslett TL, Ryan L, Bigioni T, Douketis C, Moskovits M. 1996. *Chem. Phys.* 210:343–52
98. Ren B, Lin XF, Yang ZL, Liu GK, Aroca RF, Mao BW, Tian ZQ. 2003. *J. Am. Chem. Soc.* 125:9598–99
99. Bruckbauer A, Otto A. 1998. *J. Raman Spectrosc.* 29:665–72
100. Pettinger B, Picardi G, Schuster R, Ertl G. 2002. *Single Mol.* 3:285–94
101. Pettinger B, Picardi G, Schuster R, Ertl G. 2003. *J. Electroanal. Chem.* 554/555:293-99
102. Stockle R, Suh YD, Deckert V, Zenobi R. 2000. *Chem. Phys. Lett.* 318:131–36
103. Anderson MS. 2000. *Appl. Phys. Lett.* 76:3130–32
104. Hayazawa N, Inouye Y, Sekkat Z, Kawata S. 2001. *Chem Phys. Lett.* 335:369–74
105. Nieman LT, Krampert GM, Martinez RE. 2001. *Rev. Sci. Instrum.* 72:1691–99
106. Corni S, Tomasi J. 2001. *Chem. Phys. Lett.* 342:135–140
107. Lopez-Tocon I, Centeno SP, Castro JL, Lopez-Ramirez MR, Otero JC. 2003. *Chem. Phys. Lett.* 377:111–118
108. Wu DY, Hayashi M, Tian ZQ, Lin SH. 2004. *Spectrochim. Acta*, 60A:137–146